Characterization of Micelles of Polyisobutylene-*block*-poly(methacrylic acid) in Aqueous Medium

Horst Schuch,*,† Jürgen Klingler,† Peter Rossmanith,† Thomas Frechen,† Matthias Gerst,† Jesper Feldthusen,‡ and Axel H. E. Müller*,‡,§

Kunststofflabor, BASF AG, D-67056 Ludwighafen, Germany, and Institut für Physikalische Chemie, Universität Mainz, D-55099 Mainz, Germany

Received August 31, 1999; Revised Manuscript Received December 6, 1999

ABSTRACT: Four amphiphilic block copolymers polyisobutylene-*block*-poly(methacrylic acid) (IB_m-MAA_n; $m = 70-134$, $n = 52-228$) were synthesized and transferred into aqueous medium at pH 10−12. Their structure in solution was characterized by fluorescence correlation spectroscopy (FCS), static and dynamic light scattering (SLS, DLS), analytical ultracentrifuge (AUC), and by transmission electron microscopy (TEM) with freeze-fracturing and staining techniques. DLS data, AUC sedimentation traces, and TEM images indicate at least two different kinds of particles. TEM shows spherical micelles; however, especially for polymers with larger hydrophobic blocks, additional particles are observed. FCS shows extremely low critical micelle concentrations (cmc < 0.3 mg/L). The main part of the particles consists of micelles with diameters from 15 to 50 nm, built by 130−200 block copolymer molecules. Aggregation numbers and diameters are consistent with a model recently proposed by Förster et al. (*J. Chem. Phys.* **1996**, *104*, 9956−9970). The packing densities are determined from the hydrodynamic diameters and the aggregation numbers; they vary between 6 and 32%. For large hydrophobic block lengths additional structures are found, in most cases with a narrow size distribution. The origin of these structures is discussed.

Introduction

Low-molecular-weight surfactants are widely used in emulsion polymerization to form and stabilize the polymer latex particles and to prevent coagulation of the dispersion when applied in making, for example, coatings and adhesives. The physical properties of the resulting film, however, often suffer from the presence of surfactants because they favor sensitivity to water or lower the adhesion to a substrate. In contrast, amphiphilic block copolymers are expected to overcome such disadvantages because of better compatibility with the polymer particles and a lower migration rate.

It has already been shown that block copolymers can replace surfactants to stabilize dispersions.[1,2] Additionally, block copolymers can act as blending agents to improve such properties as the mechanical strength of the resulting polymer film. Thus, the motivation of this work was to use amphiphilic block copolymers to act as a seed in emulsion polymerization to stabilize a dispersion and to create improved film properties. To cover a wide range of polymer dispersions, various hydrophilic and hydrophobic blocks have been tested. For dispersions of nonpolar polymers, polystyrene and polyisobutylene (PIB) are potential candidates, whereas poly(methacrylic acid) (PMAA) or poly(ethylene oxide) are candidates for the hydrophilic block. For this study we chose polyisobutylene-*block*-poly(methacrylic acid) (PIB-*b*-PMAA). Because PIB has a low glass transition temperature ($T_g = -55$ °C), the micelles formed in water could be expected to be dynamic, that is, exchanging single block copolymer molecules.

For a proper use, the aggregation properties of these polymers have to be known. The aggregation behavior of polymers is expected to differ from surfactants as the solvophobic and solvophilic parts of the molecule are much larger than the ones in common surfactants. The following work presents the characterization of such block copolymer micelles.

Aggregates of amphiphilic block copolymers might differ in size and architecture, for example, spheres, disks, rods, vesicles, or flocs might occur. For their analysis, fluorescence correlation spectroscopy (FCS), static and dynamic light scattering (SLS, DLS), analytical ultracentrifuge (AUC), and transmission electron microscopy were used.

Experimental Section

Synthesis of Block Copolymers. The amphiphilic block copolymers were produced by a combination of living cationic and anionic polymerizations.[3] First, isobutylene was polymerized with 2-chloro-2,4,4-trimethylpentane as the initiator and $TiCl_4$ as the catalyst in CH_2Cl_2/hexane at −78 °C. The living PIB was end-capped with diphenylethylene and quenched with methanol and ammonia to form PIB with a methoxydiphenyl terminus. Ether cleavage with K/Na alloy in tetrahydrofuran (THF) at room temperature leads to an anionic macroinitiator that was used to polymerize *tert*-butyl methacrylate (tBMA) at −20 °C. The molecular weight distribution of the PIB precursor and of PIB-*b*-PtBMA were determined by gas-phase chromatography using PIB and PtBMA standards. Subsequently the *tert*-butyl groups of the PtBMA block were hydrolyzed with hydrochloric acid in dioxane at 80 °C to form a PMAA block. Table 1 summarizes the four synthesized block copolymers with a stepwise increase of the block lengths.

Preparation of Solutions. For emulsion polymerization, block copolymer solutions with a solid content of about 3% in water have been used. To guarantee the reproducible transfer from the organic solution to the aqueous phase the following protocol was used. Five grams of the polymers with the short PIB blocks were dissolved in 50 mL of methanol. After diluting with 50 mL of water the pH was adjusted to 12 with a 0.2 N

* Authors for correspondence.
† BASF.
‡ Universität Mainz.
§ New address: Makromolekulare Chemie II, Universität Bayreuth, D-95440 Bayreuth. E-mail: axel.mueller@uni-bayreuth-.de.

10.1021/ma991491e CCC: $19.00
Published on Web 02/12/2000

Table 1. Chemical Composition and Molar Mass Averages of PIB-*b*-PMAA Copolymers Used

M_n(PIB)	$m = N_A$	M_n (PMAA)	$n = N_B$	M_n (total)	M_w/M_n
3900	70	4500	52	8400	1.06
3900	70	6000	70	9900	1.07
7500	134	12 500	145	20 000	1.04
7500	134	19 600	228	27 100	1.03

sodium hydroxide solution. Five grams of the polymers with the long PIB blocks were dissolved in 1 L of THF/water (1:1 by vol.), followed by the addition of NaOH to pH 12. The removal of the organic phase and the final concentration to 3% solids content was achieved with a rotavap under reduced pressure (70 °C, 250 mbar). In a second series, Na_2SO_4 was added to the samples (0.02 N), which reflects the situation in emulsion polymerization.

Fluorescence Correlation Spectroscopy. The experimental setup and the procedure have been described earlier.[4] The focus volume of the laser beam is about 1 μm^3. The excitation wavelength is 488 nm, fluorescence detection is at wavelengths >505 nm. The fluorescence agent, a C_{16} fatty acid with a Bodipy fluorescent dye, has a solubility of 1 nmol/L in water. In the absence of colloidal particles, this concentration leads to about one dissolved molecule within the measurement volume. After dilution of the micellar solution containing the fluorescent dye a waiting time of 24 h was used before the measurement of the fluorescence correlation time to allow excess time for establishing the thermodynamic equilibrium regarding the number of micelles.

Light Scattering. A light-scattering goniometer (ALV, Langen, Germany) with a correlator ALV 3000 was used, attached to a Nd:YAG-Laser (532 nm, 400mW; Adlas). High-quality equipment and high laser power are required in DLS for a very good signal-to-noise ratio of the autocorrelation function $g_2(\tau)$. For evaluation, both the cumulant analysis for an average hydrodynamic radius and the CONTIN algorithm are used; the latter gives the intensity distribution as a function of R_h.[5] Diameters of different colloidal species are recognized if their diameters differ by a factor of three or more. The conversion of the intensity distribution into a mass distribution would require a model for the architecture of the particle that is not available. For first estimations only spherical homogeneous particles might be assumed. The calibration of the SLS was done (a) by comparing a light-scattering intensity in the aqueous medium with that of a low-angle laser light-scattering equipment (Chromatrix KMX 6), and (b) by measuring the scattered light of nonfluorescing toluene. The solutions were cleared by a 0.45-μm filter (Millipore).

Measurements of both SLS and DLS were performed at scattering angles 30° and 90°, at a concentration of 1 g/L. This reduction of the usual Zimm analysis is reasonable because of the small interaction between the micelles [the second virial coefficient A_2 is small and the concentration of 1 g/L is well above the critical micelle concentration (cmc)] and the weak angular dependence of the scattered light. A refractive index increment of $dn/dc = 0.176$ mL/g (at 532 nm) was used for all samples. The salt content was 0.02 N Na_2SO_4 and pH 10. The exact values were found to be of no critical influence on the results.

Analytical Ultracentrifuge. The equipment and the experimental procedure are described elsewhere.[6] We used a Beckman optima XL-I AUC with an interference optical system and 12-mm double sector cells. All sedimentation velocity runs were made at 25 °C.

Transmission Electron Microscopy. ***Cryoreplica (Freeze Fracturing) Technique.*** A small drop of the block copolymer solution was shock-frozen by plunging it into liquid ethane at −120 °C. Freeze fracturing and freeze etching were carried out in a Balzers BAF 400 freeze-etching unit at a vacuum of 2×10^{-8} mbar, followed by replication with a thin evaporated Pt/C layer (5−10 nm) and backing with carbon (20 nm) for stabilization. After cleaning by floating on chromosulfuric acid, the replica was mounted on a TEM grid and imaged in a Zeiss EM 902.

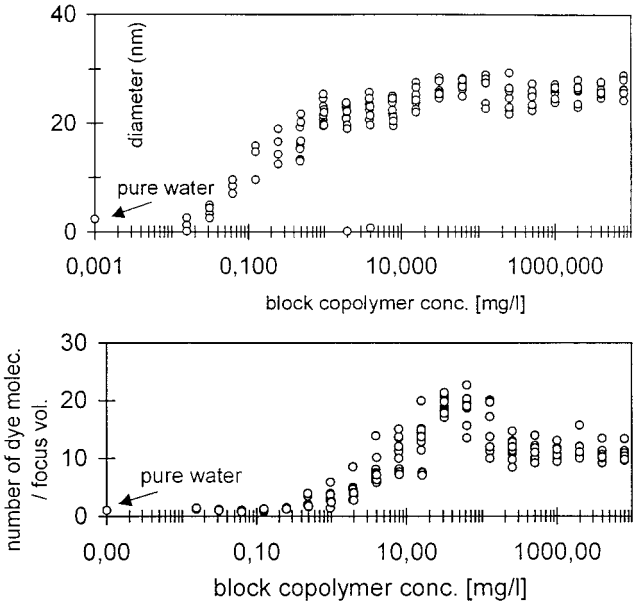

Figure 1. FCS data for IB_{70}-*b*-MAA_{52}: (a) *Hydrodynamic diameter* of the particles carrying a dye molecule as a function of the polymer concentration. The cmc is taken as the concentration where the diameter starts to increase. (b) *Number of dye molecules* in the laser focus volume as a function of the block polymer concentration: the cmc is taken as the onset of the increase of that number.

Table 2. Critical Micelle Concentrations (cmc) and Micelle Diameters, $2R_h$, Obtained by FCS

IB_m-MAA_n m/n	cmc[a] (mg/L)	cmc[b] (mg/L)	$2R_h$ (nm)
70/52	0.05	0.3	26 ± 3
70/70	0.05	0.2	26 ± 3
134/145	0.07	0.3	30 ± 3
134/288	0.10	0.3	38 ± 5

[a] From the change in the fluctuation frequency of the fluorescence intensity (change of diameter of the particles carrying labels), Figure 1a. [b] From fluctuation amplitudes of the fluorescence intensity, Figure 1b.

Staining Technique. The block copolymer solution was treated with a 2% solution of uranyl acetate, and a thin film of the solution dried on a TEM grid. Uranyl acetate stains the acidic groups of the polymer, thus revealing the shell of the micelles.

Results and Discussion

Fluorescence Correlation Spectroscopy. FCS yields the cmc; very small cmc values are accessible. In addition, the average micelle diameter, $2R_h$, is obtained from the fluctuation of the fluorescence intensity. Figure 1 and Table 2 show the FCS results. When the block copolymer concentration is increased stepwise, the particle diameter increases from the value for the single dye molecule to the value for the micelle at the cmc. When the concentration is larger than the cmc, the number of dye molecules within the laser focus volume increases because of the solubilization of dye molecules in the hydrophobic core of the micelles. For still higher concentrations, the dye fluorescence starts to be quenched. A salt content did not affect the results. The cmc of less than 0.3 mg/L is extremely small. cmc data of other amphiphilic polymers with the less hydrophobic styrene are higher. Examples: cmc = 1.6 mg/L for[7] $styrene_{37}$-*block*-EO_{236}, or cmc = 3 mg/L for[8] $styrene_{110}$-*block*-$(acrylic\ acid)_{380}$, measured by using steady-state fluorescence with pyrene as label molecule.

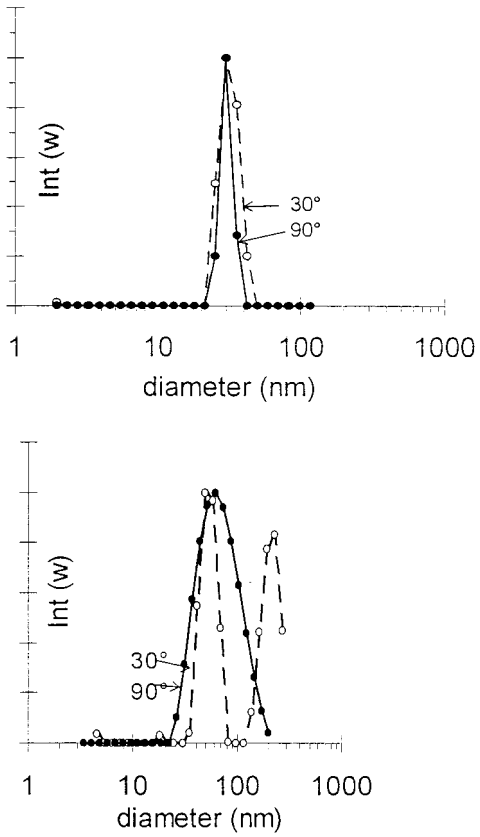

Figure 2. Particle size distribution (intensity distribution) from dynamic light scattering (DLS) by use of the CONTIN analysis at observation angles 30° and 90°. (a) IB_{70}-MAA_{70}; (b) IB_{134}-MAA_{145}; the distribution at 90° is broader than in (a); at 30° the distribution is bimodal.

Table 3. Hydrodynamic Diameters, $2R_h$ (in nm), Obtained by Dynamic Light Scattering

	$2R_h$/nm; first cumulant		$2R_h$/nm; CONTIN maxima	
IB_m-MAA_n m/n	30°	90°	30°	90°
70/52	26	27	25/90	25
70/70	31	31	30[a]	30
134/145	55	51	57/200	70[b]
134/228	120	77	58/300	100[b]

[a] Monomodal. [b] Broad distribution.

Dynamic Light Scattering. Two representative examples of particle size distributions obtained by a CONTIN analysis of DLS data are presented in Figure 2. The first example shows a unimodal distribution, independent of the scattering angle. The distribution is very narrow. The second example shows a bimodal distribution (at 30° only). Obviously the small diameters correspond to micelles; the large diameters also have a narrow size distribution, and their origin will be discussed later. The areas of the peaks correspond to the product of concentration and particle mass. Assuming a common architecture for both species, the fraction with large diameter is much less than 20% of the total mass of the sample.

The hydrodynamic diameters, $2R_h$, at the maxima of the particle size distribution and those obtained from the cumulant analysis are presented in Table 3. Obviously, the micelle diameter obtained from a cumulant analysis is useful only for monomodal samples with a narrow size distribution. For broad distributions no interpretation can be given. At a scattering angle of 30° there is a better signal-to-noise ratio available for the CONTIN analysis, which then results in bimodal distributions. The smaller diameter (bold letters) in each sample is used in the further discussions.

Table 4. Micelle Parameters Obtained by Static Light Scattering[a]

IB_m-MAA_n m/n	$M_{w,0}$	$2R_g$ (nm)	R_g/R_h	$M_w \times 10^{-6}$	Z	V_0/V
70/52	8400	<20	<0.8	1.58	188	0.32
70/70	9900	<20	<0.8	1.90	192	0.22
134/145	20 000	46	0.9	2.65	133	0.045
134/228	27 100	118	1.0	3.91	144	0.06

[a] Weight-average micellar mass, M_w, radius of gyration, R_g, aggregation number $Z = M_w/M_{w,0}$, relative packing density V_0/V (determined from M_w and $2R_h$), using the small diameter of the bimodal diameter distribution.

Static Light Scattering. The SLS experiments yield the weight-average absolute molar mass, M_w, of the micelles, The accuracy in M is 10−20%, which is important for the evaluation of the aggregation number $Z = M_w/M_{w,0}$, where $M_{w,0}$ is the molar mass of single block copolymer molecule.

The molecular weights of the colloidal particles in aqueous medium are found to be much larger than those of the single molecules. This confirms that single molecules associate to form micelles. The aggregation number covers the range $Z = 130-200$.

SLS also gives the z-averaged radius of gyration, R_g. R_g is strongly influenced by the amount of large particles. The value might be corrected because of the composition of the colloidal particles,[9] if the particle architecture is known. Here it is not known for the large particles; anyway a coarse value for R_g is sufficient for the conclusion. The uncertainty in the data is 5−10 nm, much less exact for the size characterization than the hydrodynamic radii, R_h. The ratio R_g/R_h is useful for analyzing the architecture of a particle. Because R_h determined from the first cumulant (taken at 30°) also is a z-average, these data can be directly compared. Table 4 shows that $R_g/R_h \leq 1$ for all cases. These values are consistent with (a) micelles or aggregates with a dense nucleus, (b) homogeneous spheres, or (c) hollow spheres (vesicles). They definitely do not fit to coil molecules ($R_g/R_h = 1.8$) or rods ($R_g/R_h > 2$). Hence, for the three first samples the results are consistent with micelles. For the last sample the quantity R_g/R_h may fit to a spherical arrangement of micelles or to vesicles.

The quantities $2R_h$ (from DLS) and M_w (from SLS) yield an average packing density, V_0/V, of the colloidal particles. The particles are assumed to be spheres of diameter $2R_h$, with hydrodynamic volume, $V = 4\pi/3R_h^3$. This is compared with the volume V_0 of the same amount of polymer in bulk. The relative packing density varies between 0 and 1. Alternatively, the degree of swelling can be defined as $q = V/V_0 - 1$. Table 4 shows that the packing density of these micelles is 22−32% for polymers with short hydrophobic block ($m = 70$) and 4.5−6% for the polymers with long PIB block ($m = 134$). For comparison, a polymer latex has a packing density of ca. 1, whereas a coil of a linear macromolecule has a density of below 1%. Thus, the hydrophilic polymer chains are much more extended for the large PIB blocks. The packing density represents a double average over all particles and over core and corona of each particle. Because the core is expected to have bulk density, the actual density of the corona is even smaller.

Analytical Ultracentrifuge. For the determination of the size of the micelles the proper experiment is the

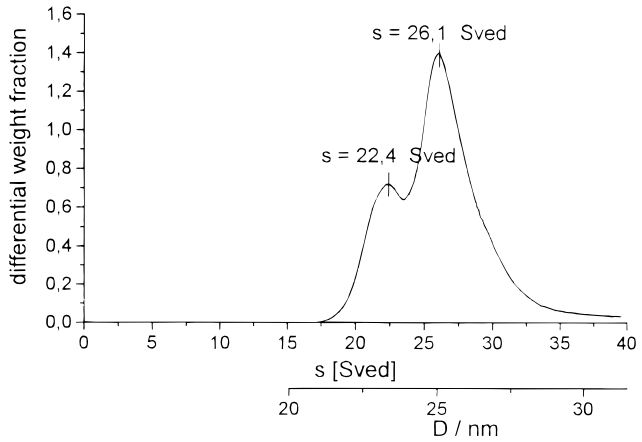

Figure 3. Distribution of the sedimentation coefficients s (in svedbergs or 10^{-13} s) for the example IB_{70}-MAA_{52}. The diameter scale is obtained by using a constant packing density V_0/V taken from DLS.

Table 5. AUC Results (Sedimentation Velocity Runs[a]

IB_m-MAA_n m/n	s_1	w_1 (%)	s_2	w_2 (%)	s_3	w_3 (%)	V/V_0
70/52			22	27	26	73	0.475
70/70			22	20	28	80	0.27
134/ 145	4.1	11	20	66	29	23	0.064
134/ 228	5.4	13	15	87			0.028

[a] Sedimentation coefficients, s_i (in svedbergs), and the corresponding mass fractions, w_i. Relative packing density, V/V_0, of the dominant component, calculated with diameter from DLS.

sedimentation velocity run. With the help of this experiment the distribution of sedimentation coefficients, *s*, is obtained (cf. Figure 3). The distributions obtained show two, and in one case even three, maxima (cf. Table 5). Obviously, there is more than one sedimenting species. The samples with shorter hydrophobic block show distributions with two maxima with a difference of only 20%.

The rather small differences of the maxima seem puzzling at first glance. Out of several explanations two are offered: (a) There are two or more kinds of micelles with different architecture and strongly different packing densities; (b) also loose aggregates of micelles exist, spherical or not. Two micelles attached to each other would sediment slightly faster than an isolated one.

The sedimentation coefficient distribution is related to the distribution of particle diameters *D* according to the Stokes equation,

$$D^2 = 18\Delta\rho\eta_{DM}s = \frac{V}{V_0}\frac{18\eta_{DM}}{\rho_P - \rho_{DM}}s$$

where η_{DM} is viscosity of the dispersing medium and ρ_{DM} and ρ_P are the densities of the dispersing medium and of the bulk polymer, respectively. The equation relates the diameter of the particle to the sedimentation coefficient via the density difference $(V/V_0)\Delta\rho = (\rho_{particle} - \rho_{DM})$. For constant sedimentation, a smaller density of the particle yields a larger diameter. If particles have the same density, differences in *D* as small as 2% are recognized by this method.

It is not possible to relate the sedimentation coefficients to hydrodynamic radii because the packing densities of the various species are not known. Thus, in reverse, the packing density of the main component was calculated by using the hydrodynamic diameter $2R_h$ obtained from DLS. The results in Table 5 show values

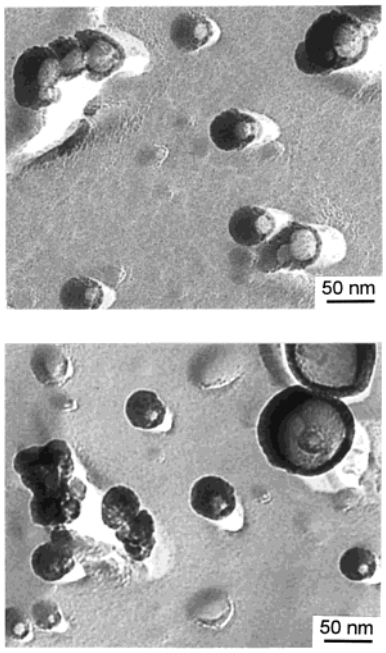

Figure 4. Transmission electron microscopy (TEM) images obtained by freeze fracturing. (a) IB_{70}-MAA_{70}; (b) IB_{134}-MAA_{228}.

of the same order of magnitude as those obtained from DLS/SLS. This helps to establish the particle architecture. The differences are within a factor of 1.3−2, the largest discrepancy relating to the sample with very low packing density.

Transmission Electron Microscopy. Representative results of cryoreplica TEM obtained by freeze fracturing are shown in Figure 4. We find small, spherical particles with diameter of 15−20 nm, considerably smaller than those obtained by FCS and DLS (cf. Table 6). In addition, much larger particles (ca. 80 nm) are observed. These partly appear as uniform spheres and partly they appear to be aggregates of small micelles. There is no dependence on the block length.

Examples of results using the staining technique are shown in Figure 5. The particle sizes are very uniform, all particles being spherical with a smooth surface. Obviously these are micelles. All samples show few aggregates—flocs with irregular shapes that probably build up during preparation. The diameters are even smaller (10−15 nm) than those observed with the cryoreplica technique and do not increase with block length; in tendency they rather decrease. However, no large particles with uniform size are observed.

The micelles most probably shrink because of the slow drying procedure. This could explain the smaller diameter compared with the freeze-fracturing technique. The differences regarding the flocs and the large uniform spherelike particles in Figure 5 compared with the results from the staining method and the influence of the preparation is not yet understood. An effect of the preparation has to be taken into account.

Comparison of Micelle Diameters Obtained by Different Techniques. Table 6 gives a survey of the results obtained by using various methods. For the one sample, DLS shows a unimodal distribution and the diameters compare well with FCS. For the other samples DLS gives two diameters. In FCS a weight-average diameter is obtained because the micelles are assumed to accept the dye molecules according to their mass. Thus, large aggregates present in small amounts will

Table 6. Comparison of Results Obtained for PIB-*b*-PMAA Block Copolymer Micelles in Aqueous Medium

	IB_m-MAA_n *m/n:*	70/52	70/70	134/145	134/228
FCS	$2R_h$ (nm)	26	26	30	38
	cmc (mg/L)	<0.3	<0.2	<0.3	<0.3
SLS	Z	188	192	133	144
	$2R_g$ (nm)	<20	<20	46	118
DLS (30°)	$2R_h$ (nm); CONTIN	25	30	57	58
	$2R_h$ (nm); 1st cumulant	26	31	55	120
SLS + DLS	R_g/R_h (1st cumulant)	<0.8	<0.8	0.9	1
	V_0/V	0.32	0.22	0.045	0.06
AUC	s (sved)[a]	26	28	20	15
AUC + DLS	V_0/V[a]	0.475	0.27	0.064	0.028
TEM	$2R$ (nm); cryoreplica[a]	-	15−20	-	15−20
	$2R$ (nm); staining	15−20	10−15	10−15	10

[a] Majority component.

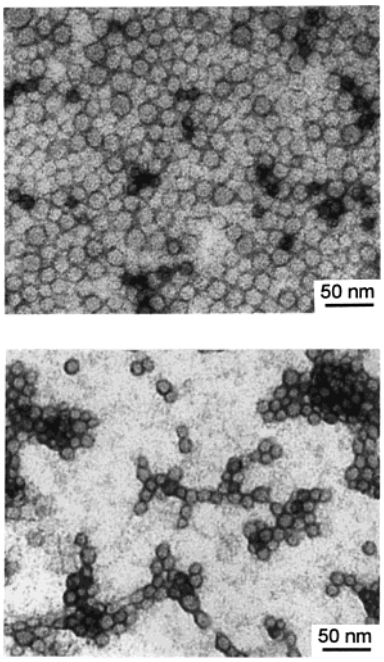

Figure 5. TEM images obtained by staining with uranyl acetate. (a) IB_{70}-MAA_{52}; (b) IB_{70}-MAA_{70}.

not be detected. In total, the combination of both methods indicates that the small diameter in light scattering is the relevant one for the micelles. The agreement between the two methods is less clear. So far one has to accept a difference of nearly a factor of 2.

AUC shows two or even three micellar species with slightly different sedimentation coefficients, the diameter of which cannot be determined. The packing densities of the main components, however, satisfactorily agree with those obtained form DLS/SLS.

TEM (staining technique) shows that there are only spherical micelles. This result is important for the choice of the model for the micellar architecture. The diameters are found to be smaller than in FCS and DLS. Probably this is due to the slow water evaporation and shrinking during sample preparation, leading to particles with packing densities close to unity. This is compatible with the results from light scattering, where the absolute masses of the micelles are not very different for different block lengths. The diameters from cryoreplica TEM are slightly larger, which is explained by the fact that during the freeze-fracturing preparation the micelle should not lose water.

Structure of Large Particles. DLS and TEM have shown that beside the "smaller" micelles there are larger particles, their fraction being less than 20% (depending on the architecture), especially for larger hydrophobic blocks. Two conjectures are offered for the architecture of the aggregates: (a) The micelles may not be in equilibrium. Because the cmc is extremely low, exchange of unimer molecules is only possible via direct contact of micelles, which may be slow. However, in this case a broader size distribution might be expected. Arrangement of the hydophobic blocks within the core is assumed to be fast because PIB has a low glass transition temperature. (b) Small-angle neutron scattering, small-angle X-ray scattering, DLS, and TEM measurements of other block copolymer micelles demonstrate the existence of superstructures:[10] clusters with regular shape, vesicles, rods, or toroids.[11] Although differing in size, the sedimentation coefficient of those could be only slightly different from the one of micelles. Our TEM results show the occurrence of large aggregates that would well fit to vesicles. The occurrence of regular superstructures would also explain the narrow size distribution for the aggregates in DLS.

A further comparison is given by single-chain surfactants, which are known to form not only micelles but also vesicles, which have a much larger size.[12] They might serve as a model for the large particles found here, being possibly nonequilibrium structures. Their amount may depend on the way of transferring the molecules from the organic into the aqueous medium.

Comparison with Theory. Because the blocks strongly differ in their water solubility, the strong segregation limit is more than reached and one expects a spherical core−shell architecture. Earlier experimental and theoretical work on this topic was reviewed by Förster et al.[13] On this basis the authors develop a more general theory that relates the quantities aggregation number, Z, the micelle diameter, $D = 2R$, and the corona thickness, D_{corona}, to the block lengths, N_A and N_B, of amphiphilic block copolymers. In the spherical core−shell model (Figure 6), the core is formed by the solvophobic chains, A. Because of the strong hydrophobic character, swelling of the core is expected to be negligible. Thus, the core density is assumed to be equal to that in bulk, that is, ca. 1 g/cm^3. The radius of the hydrophobic nucleus, R_{core}, is calculated from the amount of the hydrophobic part,

$$V_{core} = (4\pi/3)R_{core}^3 = ZV_{mol} = M_{0.4}N_AZ/\rho_A \qquad (1)$$

where V_{mol} is the molar volume of block A, and $M_{0,A}$ is the molar mass of its monomer unit. Rearrangement leads to

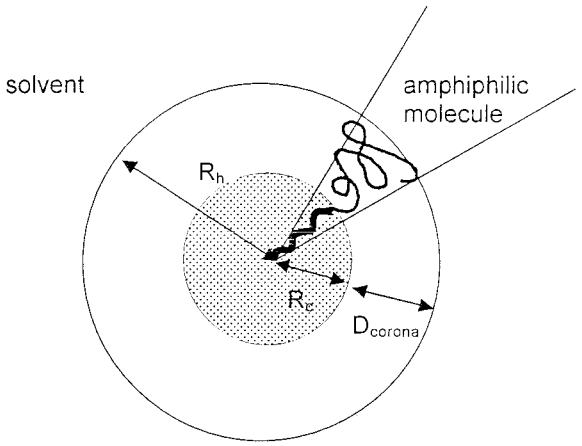

Figure 6. Micellar architecture in the strong segregation limit with one of the amphiphilic molecules drawn as a representative element of the micelle.

$$R_{core} = \left(\frac{3}{4\pi}\frac{M_{0.4}}{\rho_A}N_A Z\right)^{1/3} \quad (2)$$

The shell or corona consists of tethered solvophilic chains. The corona thickness is given by $D_{corona} = R_h - R_{core}$, where the micelle radius R_h can obtained from DLS.

According to Förster et al.[13] the aggregation number Z and the corona thickness D_{corona} are given by

$$Z = Z_0 N_A^2 N_B^{-0.8} \quad (3)$$

$$D_{corona} = D_0 Z^{0.2} N_B^{0.6} = (D_0 Z_0^{0.2}) N_A^{0.4} N_B^{0.44} \quad (4)$$

where Z_0 is in the range 0.1−0.10, and D_0 is in the range 0.2−0.3 nm.

Equations 3 and 4 show that the quantities Z and D_{corona} are influenced by both block lengths. The dominating parameter in the equation for Z is the length of the solvophobic block A. For D_{corona} the effects of the two components are comparable. There is only one fitting parameter, Z_0, in eq 3. It is related to the volume of a solvophobic monomer unit and a geometric packing parameter. Equation 4 has only one fitting parameter, D_0. It is related to the length of a solvophilic monomer unit, B, and its interaction with the solvent.

The experimental data for the reduced aggregation number and the corona thickness are plotted in Figure 7 and Figure 8. The figures include data for PMMA-*b*-PMAA and PMMA-*block*-poly(acrylic acid) obtained in another study.[14] These polymers have also shorter block lengths; the monomers are similar in the sense of the model used.

The data points for PIB-*b*-PMAA alone do not give a straightforward relation. However, together with the data for other copolymers these plots excellently describe the main trend. The values of the fitting parameters $Z_0 = 0.9$ and $D_0 = 0.24$ nm are within the expected range. This indicates that the steric arrangement dominates the micellar architecture and a relatively simple geometric model is appropriate for the IB_m-MAA_n samples consisting of 130−200 block copolymer molecules.

The micellar core shell model also raises questions about the molecular configuration. For the smaller molecules, twice their contour length is close to the experimental micellar diameter. Conjectures about their configuration are: They are less coiled than in a solvent, but rather stretched. Additionally, the shape of the core might be spherelike only when averaged over time. Also, the hydrophobic nucleus might have a hydrophilic core by inserting block copolymers with their hydrophilic part toward the center; thus a small vesicle would be formed. These conjectures are also compatible with more recent findings.[11]

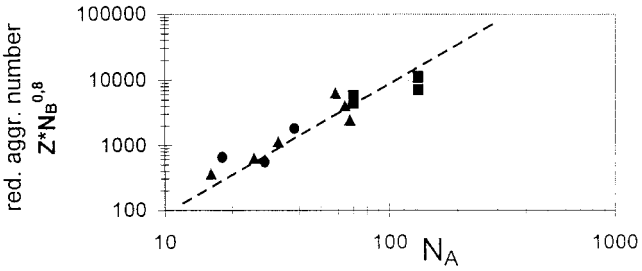

Figure 7. Reduced aggregation number, Z, of various amphiphilic block copolymers (■, PIB-*b*-PMAS; ▲, PMMA-*b*-PMAA; ●, PMMA-*b*-PAA) as function of the length N_A of the hydrophobic block. The fit uses only one fitting parameter, $Z_0 = 0.9$.

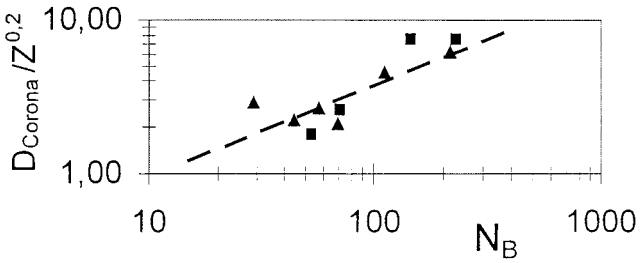

Figure 8. Reduced corona thickness of various amphiphilic block copolymers (■, PIB-*b*-PMAS; ▲, PMMA-*b*-PMAA) as function of the length N_B of the hydrophilic block. The fit uses only one fitting parameter: $D_0 = 0.24$.

For the application of these block copolymer micelles in emulsion polymerization one must remember that the aggregation number and the diameter depend on temperature and presence of monomers.[15]

Conclusions

Our comparative study shows that the various methods, FCS, DLS, SLS, AUC, and TEM supplement each other.

A part of the results was perturbed by large particles beside the micelles. The narrow size distribution of these structures and the cryoreplica TEM results point to a more regular architecture of these particles such as vesicles or well-defined spherical micellar clusters.

The spherical core−shell model of Förster et al.[13] gives a surprisingly good description of the experimental results obtained in aqueous solution and presents a quick help for choosing block lengths for the design of micelles.

Acknowledgment. Financial support from the Bundesministerium für Bildung, Wissenschaft, Forschung und Technologie, grant no. 03 N 3004, is gratefully acknowledged. We would like to thank Dr. S. Förster, Teltow, for helpful discussions.

References and Notes

(1) Riess, G.; Hurtrez, G.; Bahadur, P. Block Copolymers. In *Encyclopedia of Polymer Science and Engineering*; Mark, H. F., Bikales, N. M., Overberger, C. G., Menges, G., Kroschwitz, J. I., Eds.; Wiley: New York, 1985; Vol. 2, p. 325.

(2) Urban, D.; Gerst, M.; Rossmanith, P.; Schuch, H. *Polym. Mater. Sci. Eng.* **1998**, *79*, 440.
(3) Feldthusen, J.; Iván, B.; Müller, A. H. E. *Macromolecules* **1997**, *31*, 578.
(4) Klingler, J.; Friedrich, T. *Biophys. J.* **1997**, *73*, 2195.
(5) Schmidt, M. In *Dynamic Light Scattering*; Brown, W., Ed.; Clarendon: Oxford, 1993; pp 372−406.
(6) An overview is given in *Analytical Ultracentrifugation in Biochemistry and Polymer Science*; Harding, S. E., et al., Eds., Royal Society of Chemistry: Cambridge, 1992; Chapter 10.
(7) Wilhelm, M.; Zhao, C.-L.; Wang, Y.; Xu, R.; Winnik, M. A.; Mura, J.-L.; Riess, G.; Croucher, M. D. *Macromolecules* **1991**, *24*, 1033.
(8) Astafieva, I.; Zhong, X. F.; Eisenberg, A. *Macromolecules* **1993**, *26*, 7339.
(9) See, for example, Kratochvil, P. *Classical Light Scattering of Polymers*; Amsterdam, 1987.
(10) (a) Zhang, L.; Eisenberg, A. *Science* **1995**, *268*, 1728. (b) Yu, K.; Zhang, A.; Eisenberg, A. *Langmuir* **1996**, *12*, 5980. (c) Yu, K.; Eisenberg, A. *Macromolecules* **1996**, *29*, 6359.
(11) Förster, S. Private communication.
(12) Hoffmann, H.; Grabner, D.; Hornfeck, U.; Platz, G. *J. Phys. Chem. B* **1999**, *103*, 611.
(13) Förster, S.; Zisenis, M.; Wenz, E.; Antonietti, M. *J. Chem. Phys.* **1996**, *104*, 9956−9970.
(14) Schuch, H.; Klingler, J.; Rossmanith, P.; Frechen, T.; Gerst, M.; Müller, A. H. E.; Stauf, W. To be published.
(15) Liu, T.; Schuch, H.; Gerst, M.; Chu, B. *Macromolecules* **1999**, *32*, 6031.

MA991491E